Classical treatment of the electron emission from collisions of uracil molecules with fast protons

L. Sarkadi*

Institute for Nuclear Research of the Hungarian Academy of Sciences (MTA Atomki), P.O. Box 51, H-4001 Debrecen, Hungary

(Received 19 October 2015; published 8 December 2015)

The electron emission from the uracil molecule induced by fast proton impact has been investigated using the classical-trajectory Monte Carlo (CTMC) method. Applying the independent-particle model, the full three-body dynamics of the projectile, an active electron, and the molecule core is considered. The interactions with the molecule core are described by a multicenter potential built from screened atomic potentials. Double and single differential, as well as total ionization cross sections are calculated and compared with the predictions of the first Born approximation with correct boundary conditions (CB1), the continuum-distorted-wave–eikonal-initial-state (CDW-EIS) approach, as well as the combined classical-trajectory Monte Carlo–classical over-the-barrier (CTMC-COB) model. The effect of the molecular treatment of the ionization by the multicenter potential is analyzed by simplified CTMC calculations in which the ionization cross section of the uracil is determined as a linear combination of the contributions of the constituent atoms of the molecule.

DOI: 10.1103/PhysRevA.92.062704 PACS number(s): 34.50.Gb, 34.10.+x

I. INTRODUCTION

An increasing number of studies have been devoted recently to reveal the properties of the ionization processes induced in molecules of biological importance by the impact of fast particles. The great interest is mainly explained by the potential applications of the results (radiation protection, medical imaging, proton therapy, etc.). Besides the applications, the understanding of the ionization of large molecules is itself a problem of fundamental importance.

Besides water, the DNA–RNA nucleobases are the more frequently used molecules as targets in the collisional investigations involving bio-molecules. This is explained by their important role in the processes that lead to damages induced by the ionizing radiation in the biological medium.

The present work deals with the ionization of the RNA base molecule, *uracil* ($C_4H_4N_2O_2$), by impact of fast protons. In the past 10–15 years the collisional interaction of this molecule with ions has been the subject of a number of experimental and theoretical investigations. In most of the experimental works [1–5] total and partial cross sections have been measured for ionization, fragmentation, and charge transfer by impact of protons and heavier ions (C, O, and F) of different charge states in a broad range of the collision energy, from a few keV/amu up to a few MeV/amu. Differential investigations have been reported only by two research groups. Moretto-Capelle and Le Padellec [6] carried out an electron spectroscopic measurement for the electron emission from gas-phase uracil molecules due to collisions with protons in the 25- to 100-keV energy range. They determined absolute double-differential cross sections (DDCSs) at 35° emission angle. Recently, Itoh *et al.* [7] have measured absolute DDCSs for the process at 0.5-, 1.0-, and 2.0-MeV proton energies. The range of the electron energy and the emission angle covered by their experiment was 1–1000 eV and 15°−165°, respectively.

On the theoretical side, classical, semiclassical, and fully quantum mechanical models have been applied for the description of the ion-uracil collisions. Bacchus-Montabonel [8] *et al.* treated the charge transfer from uracil to low-velocity ($v < 1$ a.u.) C^{q+} ions ($q = 2 - 4$) by means of *ab initio* quantum-chemical molecular methods. The authors employed the impact parameter formalism for the description of the collisional dynamics. Moretto-Capelle and Le Padellec [6] used the classical-trajectory Monte Carlo (CTMC) method for the interpretation of their experimental DDCS results obtained for proton on uracil collisions. Lekadir *et al.* [9] calculated single-electron ionization and single-electron capture cross sections for the collisions of H^+, He^{2+}, and C^{6+} ions with DNA–RNA nucleobasis (including uracil) at impact energies ranging from 10 keV/amu to 10 MeV/amu in the framework of another classical approach, namely the CTMC-COB model. The latter model combines several features of CTMC and the classical over-the-barrier (COB) description [10]. As far as the quantum mechanical description is concerned, two models have been proposed [11,12]. One is the first Born approximation with correct boundary conditions (CB1), which originally had been suggested by Belkić *et al.* [13] for the treatment of the electron capture in ion-atom collisions. The other is the continuum-distorted-wave–eikonal-initial-state (CDW-EIS) approach [14].

The quantum mechanical models provided DDCS values in a reasonable agreement with the DDCS data measured by Itoh *et al.* [7] for uracil at 1-MeV proton impact, except for electron energies below 10 eV. In this energy range both models predict slightly increasing DDCS with decreasing energy, while the measured data show a strongly decreasing tendency. The disagreement with the measurements is smaller at larger observation angles. As a possible explanation, Champion *et al.* [12] attributed the observed discrepancy between the theory and experiment to secondary collisions of the primarily ejected low-energy electrons on the surrounding atomic centers during their flight inside the molecule. Since both quantum mechanical models consider the ionization of the molecule as a linear combination of *atomic* ones, they cannot give an account of multiple scattering effects.

One of the motivations of the present work was the above-mentioned discrepancy. It was an interesting question whether the application of a *multicenter* molecular potential in the ionization models resolves the discrepancy and improves

*sarkadil@atomki.hu

the agreement between the theory and experiment. As an ionization model, we chose CTMC. While the inclusion of multicenter potential into the quantum mechanical models gives rise to serious difficulties in the solution, it is straightforward and relatively easy for CTMC. Another motivation was the poor agreement between the CTMC results of Moretto-Capelle and Le Padellec [6] and their DDCS data measured at 100-keV proton energy. Their calculations carried out with a multicenter molecular potential overestimated the experimental DDCS values at an average by a factor of 1.75. Even larger deviations, reaching two orders of magnitude at low electron energies, were observed between their experimental data and the calculations of Galassi *et al.* [11] made in the framework of both quantum mechanical models, CB1 and CDW-EIS.

The organization of the paper is as follows. In Sec. II, we outline the model with particular emphasis on the construction of the multicenter atomic potential. Furthermore, we present our procedure for the generation of the initial position and momentum coordinates of the electron in the case of the anisotropic molecular potential. In Sec. III, we compare the calculated differential and total ionization cross sections with existing experimental data and the predictions of other theoretical models, including the results obtained by a simplified CTMC procedure in which the ionization cross section of the uracil is determined as a linear combination of the contributions of the constituent atoms of the molecule.

Atomic units are used throughout the paper, unless otherwise indicated.

II. THEORETICAL METHOD

Assuming the validity of the independent particle model (IPM), we applied a three-body CTMC approach that considers the interaction between the projectile, an active electron, and the ion core of the molecule. The CTMC method is based on the numerical solution of the classical equations of motion for a large number of trajectories of the interacting particles under randomly chosen initial conditions [15,16].

The present CTMC computer code worked out for the description of the ion-molecule collisions is based on a previous code used for ion-atom collisions (for details see Ref. [17]). It solves Newton's nonrelativistic equations of motion for the three particles:

$$m_i \frac{d^2\mathbf{r}_i}{dt^2} = \sum_{j(\neq i)=1}^{3} \mathbf{F}_{ij}(\mathbf{r}_i - \mathbf{r}_j), \quad (i = 1,2,3). \tag{1}$$

Here m_i and $\mathbf{r}_i$ are the masses and the position vectors of the three particles, respectively. Introducing the notations e, P, and T for the electron, projectile, and target, the $\mathbf{F}_{ij}$ forces in (1) are the e-P, e-T, and P-T interactions. The e-T force is determined as $-\nabla_{\mathbf{r}_{ij}} V_{\rm mod}(\mathbf{r}_{ij})$, where $\mathbf{r}_{ij} = \mathbf{r}_i - \mathbf{r}_j$ is the relative position vector of the two particles. $V_{\rm mod}(\mathbf{r})$ is a multicenter *model* potential that describes the interaction of the active electron in the mean field created by the nuclei and the rest electrons of the molecule. For a bare ion projectile of charge $Z_{\rm P}$ the P-T force is derived similarly: $-Z_{\rm P}\nabla_{\mathbf{r}_{ij}}[-V_{\rm mod}(\mathbf{r}_{ij})]$. The e-P interaction in this case is Coulombic.

Realistic multicenter molecular potential can be obtained from quantum chemical calculations (see, e.g., Ref. [6]). Instead, we apply a simple method introduced in our previous work [18] in which we investigated the electron emission from H_2O and CH_4 by impact of fast ions, both experimentally and theoretically. One of the applied theoretical models was CTMC. In the CTMC calculations for H_2O target we used $V_{\rm mod}(\mathbf{r})$ obtained by Illescas *et al.* [19] by means of quantum chemical calculations. Such potential for CH_4 was not available in the literature, so we looked for a simple way how to construct it. Analyzing the form of $V_{\rm mod}(\mathbf{r})$ proposed by Illescas *et al.* for H_2O, we arrived at the idea that $V_{\rm mod}(\mathbf{r})$ can be well approximated by the sum of screened atomic potentials.

The details of our procedure are given in Ref. [18]. Briefly, for a screened atomic potential one may use the Green-Sellin-Zachor potential [20]:

$$V^{\rm GSZ}(r) = -\{Z - (N-1)[1 - \Omega(r,\eta,\xi)]\}/r, \tag{2}$$

where Z is the nuclear charge, N is the number of the electrons in the ion, and

$$\Omega(r,\eta,\xi) = \{(\eta/\xi)[\exp(\xi r) - 1] + 1\}^{-1}.$$

η and ξ are parameters that depend on N and Z.

$V^{\rm GSZ}(r)$ can be written as a sum of long- and short-range potential:

$$V^{\rm GSZ}(r) = -\frac{Z - (N-1)}{r} - \frac{(N-1)}{r}\Omega(r,\eta,\xi). \tag{3}$$

In the molecule the potentials at the atomic centers differ from those of the isolated atoms. In Ref. [18] we have shown that the change of the atomic potential at a molecular center can be well expressed by the change of the electron number from N to $N + \Delta N$. In this way, a constituent atom A of the molecule contributes to $V_{\rm mod}(\mathbf{r})$ with the following potential,

$$V_{\rm A}^{\rm GSZ}(r_{\rm A}) = -\frac{Z_{\rm A} - (N_{\rm A} - \Delta N_{\rm A} - 1)}{r_{\rm A}} - \frac{N_{\rm A} - \Delta N_{\rm A} - 1}{r_{\rm A}} \times \Omega(r_{\rm A},\eta_{\rm A},\xi_{\rm A}). \tag{4}$$

Here $r_{\rm A}$ is the distance of the electron from the nucleus of the atom A.

For the water molecule we found that by suitable choice of $N_{\rm A}$ and $\Delta N_{\rm A}$ for the oxygen and hydrogen centers one can obtain the same coefficients of the short-and long-range parts of the above potential as those of the center potentials in $V_{\rm mod}(\mathbf{r})$ given by Illescas *et al.* Furthermore, it turned out that excellent agreement between the latter potential and that constructed from the screened atomic potentials can be obtained even in the "zeroth-order approximation," i.e., assuming $\Delta N_{\rm A} = 0$ for both atoms. In Ref. [18] for the CH_4 molecule we used the zeroth-order approximation for the construction of the five-center potential. Our CTMC calculations carried out with this potential for the ionization of CH_4 by 1-MeV proton and He^+ projectiles resulted in DDCS values in very good agreement with the experimental data.

For the uracil molecule we constructed the multicenter potential along the same line as for H_2O and CH_4. It has

the form,

$$V_{\text{uracil}}(\mathbf{r}) = \sum_{i=1}^{n_{\text{H}}} V_{\text{H}}(r_{\text{H}i}) + \sum_{i=1}^{n_{\text{C}}} V_{\text{C}}(r_{\text{C}i}) + \sum_{i=1}^{n_{\text{N}}} V_{\text{N}}(r_{\text{N}i}) + \sum_{i=1}^{n_{\text{O}}} V_{\text{O}}(r_{\text{O}i}). \quad (5)$$

Here $r_{\text{A}i}$ is the distance of the electron from the nucleus of the ith A atom, and n_{A} is the number of the A atom in the molecule. $V_{\text{A}}(r_{\text{A}})$ is approximated by the modified Green-Sellin-Zachor potential given by Eq. (4), $V_{\text{A}}(r_{\text{A}}) \approx V_{\text{A}}^{\text{GSZ}}(r_{\text{A}})$. In our calculations the parameters η_{A} and ξ_{A} were taken from Garvey *et al.* [21].

$V_{\text{A}}^{\text{GSZ}}(r_{\text{A}})$ is parametrized as follows. For each atom $N_{\text{A}} = Z_{\text{A}} + 1$. For the hydrogen atoms $\Delta N_{\text{H}} = 0$. The asymptotical behavior of the multicenter potential,

$$V_{\text{uracil}}(r \to \infty) = -\frac{1}{r}, \quad (6)$$

is ensured by the choice $\Delta N_{\text{A}} = 1/(n_{\text{C}} + n_{\text{N}} + n_{\text{O}})$ for the carbon, nitrogen, oxygen atoms. The choice $\Delta N_{\text{H}} = 0$ can be justified by the small corresponding value found for water. The equivalent treatment of the heavy atoms is based on the picture that the ionization takes place mostly from loosely bound molecular orbitals that are highly delocalized, therefore one cannot expect large differences among the contributions of the atoms to the asymptotical unit charge.

It is important to note that at each atomic center in the limit $r_{\text{A}} \to 0$ Eq. (4) leads to the potential of the bare nuclear charge:

$$V_{\text{A}}(r_{\text{A}}) = -\frac{Z_{\text{A}}}{r_{\text{A}}}. \quad (7)$$

The anisotropic molecular potential gives rise to a further difficulty in CTMC, namely that the generation of the initial values of the position and momentum coordinates of the electron is more complicated than that for the isotropic atomic potential. For the latter case Reinhold and Falcón [22] suggested a general method. In Ref. [18] we extended their method for the case of anisotropic potentials. Briefly, the central quantity in the original procedure of Reinhold and Falcón is the integral,

$$\omega(r) = \int_0^r dr' \mu r'^2 \{2\mu[E_i - V(r')]\}^{1/2}. \quad (8)$$

Here $E_i = p^2/2\mu + V(r)$ is the binding energy of the electron, $\mu = m_{\text{T}}/(1 + m_{\text{T}})$. The range of the radial distance of the electron is confined to the interval $0 < r < r_0$ because of the condition that the kinetic energy is positive. The maximum value r_0 is obtained as the root of the equation,

$$E_i - V(r) = 0. \quad (9)$$

The first step to determine the initial r value is the random choice of ω in the interval $[0,\omega(r_0)]$. Once a value of ω is chosen, r is obtained from the inverse of the $\omega(r)$ function.

For *anisotropic* potential we modified the integral (8) in the following way:

$$\omega(r,\theta_r,\phi_r) = \int_0^r dr' \mu r'^2 \{2\mu[E_i - V(r',\theta_r,\phi_r)]\}^{1/2}, \quad (10)$$

where θ_r and ϕ_r are the polar angles of the position vector $\mathbf{r}$. In this case the procedure starts with the selection of the direction of $\mathbf{r}$ by random choice of $\nu_r = \cos\theta_r$ in the interval $[-1,1]$, and ϕ_r in the interval $[0,2\pi]$. Then the equation,

$$E_i - V(r,\theta_r,\phi_r) = 0, \quad (11)$$

has to be solved at the selected (θ_r,ϕ_r) direction. Now the root $r_0 = r_0(\theta_r,\phi_r)$. Again, after the random choice of an ω value with the condition $0 < \omega < \omega[r_0(\theta_r,\phi_r)]$, r is obtained from the inverse of the $\omega(r,\theta_r,\phi_r)$ function given by Eq. (10).

Once r is known, the components of the momentum vector are calculated as

$$\begin{aligned} p_x &= \{2\mu[E_i - V(r,\theta_r,\phi_r)]\}^{1/2}\left(1-\nu_p^2\right)^{1/2}\cos\phi_p, \\ p_y &= \{2\mu[E_i - V(r,\theta_r,\phi_r)]\}^{1/2}\left(1-\nu_p^2\right)^{1/2}\sin\phi_p, \\ p_z &= \{2\mu[E_i - V(r,\theta_r,\phi_r)]\}^{1/2}\nu_p. \end{aligned} \quad (12)$$

Here ν_p and ϕ_p are randomly selected in the interval $[-1,1]$ and $[0,2\pi]$, respectively.

While the procedure outlined above was applied successfully for H_2O and CH_4, it failed for uracil. It turned out that it can be used only for potentials characterized by a small degree of anisotropy ("quasi-isotropic" potentials). Since for both H_2O and CH_4 the molecular potential is dominantly determined by that of the heavy atom, its spatial distribution is almost spherically symmetric. At the same time, the potential of uracil is highly anisotropic because of the planar ring structure of the molecule. The failure of the presented procedure for uracil is explained by the lack of *weighting* of the different directions along which the integration in (10) is carried out. The latter integral provides normalized distributions at all selected directions. As a weighting procedure, it is plausible to assume that the probability of finding an electron at a given (θ_r,ϕ_r) direction is proportional to the volume of the integration at the maximum radial distance, $\Delta V \propto r_0^3(\theta_r,\phi_r)$. By denoting the *global* r_0 value (i.e., the maximum among the r_0 values considering all directions in the molecule at a fixed value of the binding energy) by R_0, the weighting factor is $r_0^3(\theta_r,\phi_r)/R_0^3$. This so-called "volume" correction was implemented in the CTMC code by introducing a random variable χ with uniform distribution in the interval $[0,1]$. For the random generation of r at a given (θ_r,ϕ_r) direction the criterion of the acceptance of a trial event: $\chi \leqslant r_0^3(\theta_r,\phi_r)/R_0^3$.

For the uracil molecule one is faced with a further complication, namely that below a certain binding energy Eq. (11) can have more than one root. For the potential given by Eq. (5) this energy is -1.155 a.u. In our CTMC calculations we considered 29 molecular orbitals (MOs), with binding energies ranging from -0.349 a.u. to -19.71 a.u. [11]. For the first 17 MOs Eq. (11) has one root, for the rest MOs the number of the roots can be one, two, or three. In calculation of the initial electron coordinates only those domains of the molecule were considered, where the kinetic energy of the electron is positive.

In Figs. 1 and 2 the contour map of the initial electron position obtained by the above procedure is shown for a loosely and a strongly bounded electron, respectively. With increasing binding energy the electron is more and more localized at the atomic centers, as it is expected. The delocalized motion of

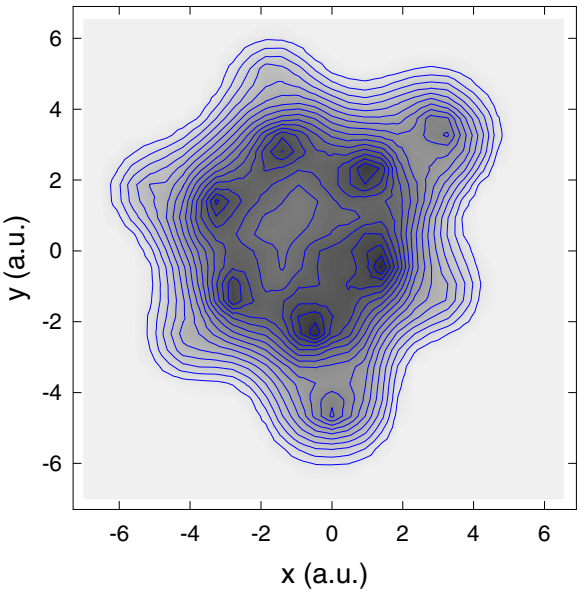

FIG. 1. (Color online) Contour map of the initial electron position in uracil. The binding energy of the electron is −0.581 a.u. x and y are coordinates of the projection of the position vectors into the molecule plane. From light to dark the intensity level increases linearly.

the electron in case of small binding energy is demonstrated by the plot of a typical electron trajectory in Fig. 3.

We emphasize that our method to generate the initial values of the position and momentum coordinates of the electron is based on some physical considerations, it is not an exact procedure. In this context the question arises how far the results of the CTMC calculations depend on the applied procedure. Intuitively one feels that in the ideal case the initial position and momentum distribution remains constant in time

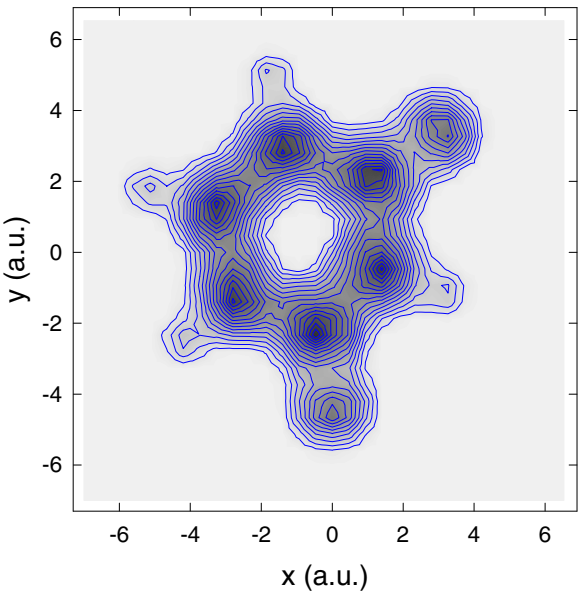

FIG. 2. (Color online) The same as Fig. 1, but the binding energy of the electron is −1.385 a.u.

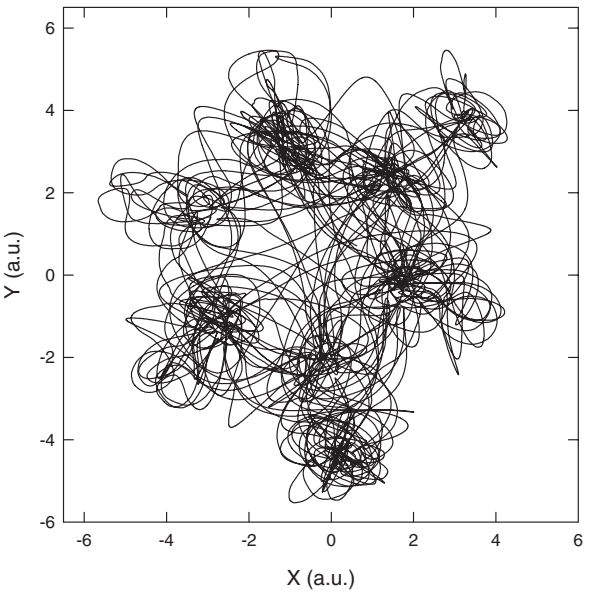

FIG. 3. An example of the electron trajectory in the uracil molecule (projection into the plane of the molecule). Binding energy, −0.581 a.u.

(in the absence of outer forces), i.e., it is identical to the equilibrium (relaxed) distribution. Figure 4 shows the electron radial distance distribution in uracil initially and after a time of 10^3 a.u. calculated with neglect of the interactions with the projectile. According to the figure, the initial distribution is almost the same as the relaxed one. This result proves the correctness of the procedure applied in the present work.

For a noncoincidence experiment the measured cross section is an average of the contributions from randomly oriented molecules. To make a comparison with the experiment, the theory has to consider also the random orientation of the molecules. This was achieved in the present work by the random rotation of the molecule using the three Euler angles at

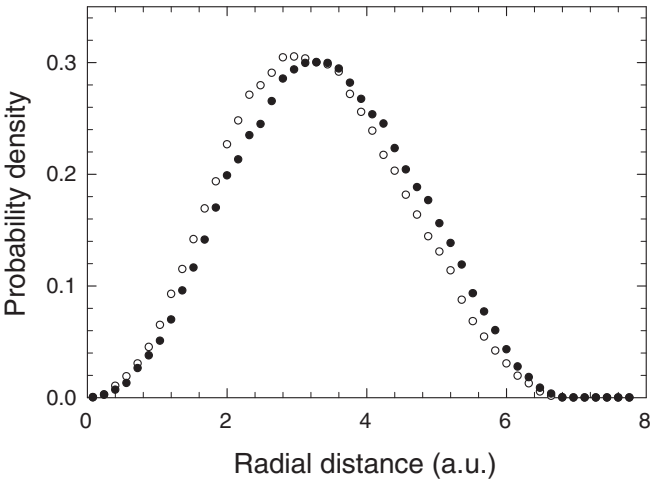

FIG. 4. The probability density function of the electron radial distance in uracil initially (open circles) and after a time of 10^3 a.u. (solid circles). The interactions with the projectile are switched off. The binding energy of the electron is −0.581 a.u.

each collision event. By a suitable transformation of the Euler angles to uniformly distributed random variables we ensured the isotropic distribution of the molecule orientation.

The double differential cross section (DDCS) for the electron production describing the energy and angular distribution of the electron following the ionization of the molecule is calculated as the sum of DDCSs for the electron emission from the individual MOs:

$$\frac{d^2\sigma}{d\epsilon\, \mathrm{d}\Omega} = \sum_{i=1}^{N_{\mathrm{MO}}} \frac{d^2\sigma_i}{d\epsilon\, \mathrm{d}\Omega}, \tag{13}$$

where N_{MO} is the number of the MOs. For a given MO, classically the DDCS can be expressed as (omitting the subscript i)

$$\frac{d^2\sigma}{d\epsilon\, \mathrm{d}\Omega} = n\, 2\pi \int_0^\infty b\, \frac{d^2p}{d\epsilon\, \mathrm{d}\Omega}(b)\, db, \tag{14}$$

where $d^2p/d\epsilon\, d\Omega$ is the *one-electron* double-differential ionization probability for the regarded MO, n is the number of the electrons in the MO, and b is the impact parameter. We note here that the above expression can be applied only for electron emission having azimuthal symmetry. Although this is not the case for a molecule of a *fixed* orientation, for the averaged emission of randomly oriented molecules the condition of the azimuthal symmetry is fulfilled.

For a large number of collision events characterized by uniformly distributed b values in the range $(0, b_{\max})$ the integral in (14) can be approximated by the following sum:

$$\int_0^\infty b\, \frac{d^2p}{d\epsilon\, \mathrm{d}\Omega}(b)\, db \approx \frac{b_{\max} \sum_j b_j}{N_{\mathrm{tot}} \Delta\epsilon\, \Delta\Omega}. \tag{15}$$

Here b_j is the actual impact parameter at which the electron is emitted with energy and angle that falls in the energy window $\Delta\epsilon$ and solid angle window $\Delta\Omega$, and N_{tot} is the total number of the collision events. $\Delta\Omega$ is determined by the polar angular window ranging from $\theta_{\min}$ to $\theta_{\max}$:

$$\Delta\Omega = \int_0^{2\pi} \int_{\theta_{\min}}^{\theta_{\max}} \sin\theta\, d\theta\, d\phi = 2\pi(\cos\theta_{\min} - \cos\theta_{\max}). \tag{16}$$

From Eqs. (15) and (16) we obtain for a given MO,

$$\frac{d^2\sigma}{d\epsilon\, d\Omega} \approx n \frac{b_{\max} \sum_j b_j}{N_{\mathrm{tot}}(\cos\theta_{\min} - \cos\theta_{\max})\, \Delta\epsilon}. \tag{17}$$

Besides DDCSs, in the present work we determined also *single* differential cross sections (differential with respect to the electron energy, SDCS) and *total* cross sections (TCS) for the electron emission. The contribution of a given MO to SDCS and TCS is expressed as

$$\frac{d\sigma}{d\epsilon} \approx n\, 2\pi \frac{b_{\max} \sum_j b_j}{N_{\mathrm{tot}} \Delta\epsilon}, \tag{18}$$

and

$$\sigma \approx n\, 2\pi \frac{b_{\max} \sum_j b_j}{N_{\mathrm{tot}}}, \tag{19}$$

respectively.

Further details of the calculations are as follows. Assuming the validity of the Franck-Condon approximation, the calculations are carried out at fixed, equilibrium geometry of the uracil molecule. The Cartesian coordinates of the gas phase molecule were taken from Ref. [23]. As a check, using the coordinates we calculated the bond lengths and bond angles of the molecule. The obtained values were found in good agreement with the experimental and theoretically calculated bond lengths and bond angles (see, e.g., Ref. [24]). We considered 29 MOs of the uracil. As binding energies and electron population numbers we used the data obtained by Galassi *et al.* [11] by *ab initio* quantum chemical calculations.

The integration of the equations of motion was started at such a large distance R_0 between the incoming proton and the uracil molecule at which the relative change of the binding energy of the electron due to the perturbation by the projectile in the considered MO was less than 10^{-4}. After the collision the calculations were made in two steps. In the first step the integration was continued until the proton receded to the same distance as that of the initial approach R_0. This distance was large enough to identify the main reaction channels (excitation, ionization, and charge transfer). In the second step only collision events leading to ionization were regarded, and the trajectories of the particles were calculated up to $R = 10^3$ a.u.

In the present investigations we followed the history of altogether 8.61×10^8 collision events.

III. RESULTS AND DISCUSSION

In Fig. 5 the DDCS values obtained by our CTMC method for the ionization of uracil by impact of 1-MeV protons are compared with the experimental data [7] and the results of CDW-EIS and CB1 calculations [12]. According to the figure, CTMC provides a reasonable description of the process. However, CTMC could not resolve the discrepancy between the theory and experiment observed below 10-eV electron energy. As it was mentioned in the Introduction, Champion *et al.* [12] attributed the discrepancy to secondary collisions of the primarily ejected low-energy electrons on the surrounding atomic centers during their flight inside the molecule. Unlike CDW-EIS and CB1, our CTMC applies a multicenter molecule potential, therefore, in principle, it gives an account of such secondary scattering effects. The fact that CTMC is in almost perfect agreement with the other two models for electron energies of a few eV indicates that the contribution of the secondary scatterings to the electron emission is very small, and thereby it rules out the explanation by the above authors.

A further conclusion that can be drawn from Fig. 5 is that the CTMC results give strong support to the CB1 model. The fact that both CTMC and CB1, these two completely different theoretical approaches, describe the experimental data equally well (above 10 eV) support the correctness of the measurement and indicates that the increasing deviations seen between CDW-EIS and the experiment with increasing emission angle and energy at backward direction are due to the bad performance of the applied CDW-EIS model.

The worst agreement between CTMC and the experiment occurs at 15° at electron energies covering the range of the C, N, and O K-LL Auger peaks. CTMC predicts a bumplike structure in this energy range. Since the theory does not include the Auger electron emission, it is expected to describe only the "background" under the peaks. One may attribute the bump

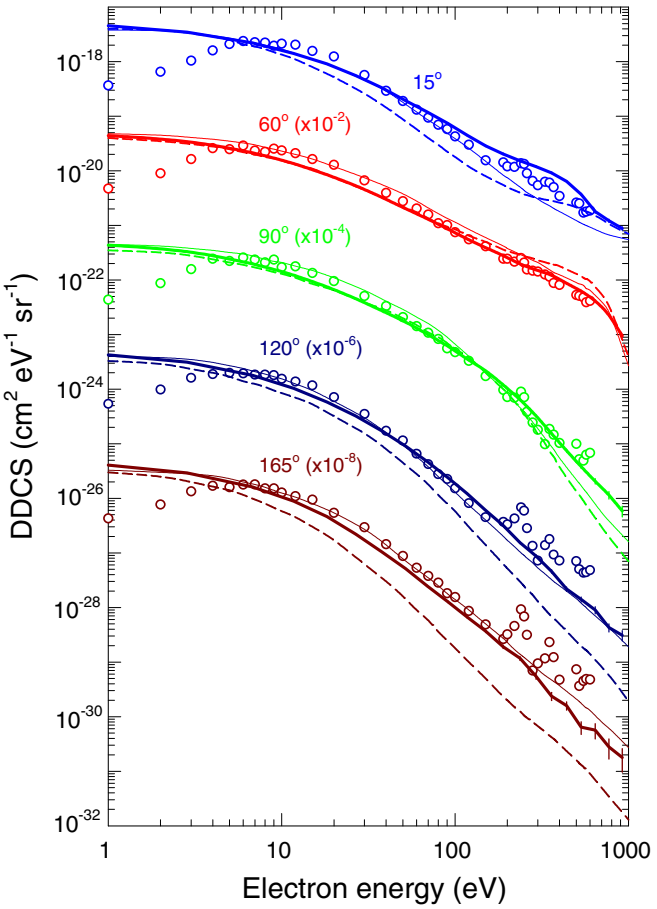

FIG. 5. (Color online) Double-differential cross section for the electron emission from the uracil molecule following ionization by 1-MeV proton impact. Open circles, measured data [7]; dashed line, CDW-EIS [12]; thin solid line, CB1 [12]; thick solid line with error bars, present CTMC.

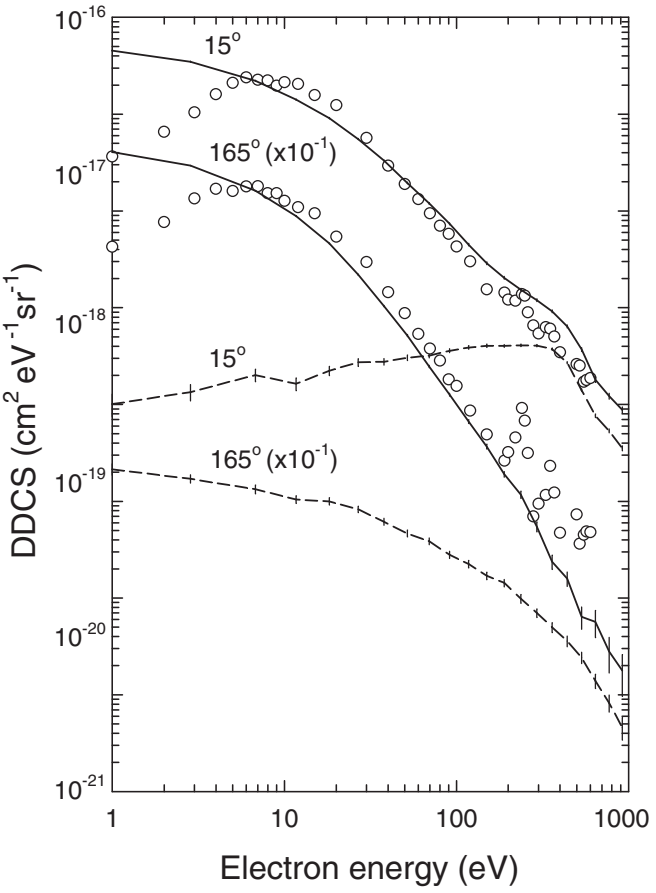

FIG. 6. The contribution of the ionization of inner MOs of the uracil molecule (dashed lines) to the total DDCS (solid lines). The impact energy is 1 MeV; the experimental data are the same as in Fig. 5.

to the ionization of the inner MOs of the molecule (the K shells of the heavy atom constituents) whose contribution to the total DDCS increases with increasing electron energy. Indeed, the DDCS for the ionization of inner MOs shows a broad maximum at about 300 eV, as is seen in Fig. 6. We note that CDW-EIS also predicts a bump, but at somewhat higher energy, about 500 eV (see Fig. 5). Moreover, the concave shape of the CB1 curve above 100 eV indicates the presence of a structure at even higher electron energy. However, the latter one is most likely the binary encounter peak whose expected energy is $4\,(m_e/m_p)\,E_p\,\cos^2(\theta) = 2032$ eV.

Larger deviations between CTMC and experiment are observed also at 165° above 300 eV, where CTMC underestimates the measured DDCS data. According to Fig. 6, the contribution of the inner MOs is small here. We note, however, that in this case the comparison between the theory and experiment is uncertain because of the large statistical error of the CTMC results. From the experimental side, the long Lorentz tails of the Auger peaks do not allow an accurate determination of the DDCS. More reliable cross sections could be obtained by extending the energy range of the measurements well above the Auger peaks.

In Fig. 7 the present SDCS results for 1-MeV impact energy are compared with the experimental data and the predictions of the two quantum mechanical models as a function of the electron energy. Above 100 eV CTMC is in perfect agreement with the experiment and CB1. At lower energies CTMC predicts SDCS values that lie between those obtained by CB1 and CDW-EIS.

As it was mentioned in the Introduction, the present study was also motivated by the poor agreement between the CTMC results of Moretto-Capelle and Le Padellec [6] and their DDCS data measured at 100-keV proton energy, as well as the discrepancy of two orders of magnitude observed between their experimental data and the CB1 and CDW-EIS calculations of Galassi *et al.* [11]. According to Fig. 8 our CTMC results support the latter calculations. Although the present CTMC predicts slightly smaller DDCS values than CB1 and CDW-EIS, the difference between the two CTMC results is still very large. Furthermore, our calculations do not show the peak appearing at 20 eV in case of the calculations of Moretto-Capelle and Le Padellec.

In Fig. 9 the total (integrated) electron emission cross sections obtained in the present work are compared with the results of other theories (CDW-EIS and CB1 [12], CTMC-COB [9]) and with the available experimental data [3,7] as

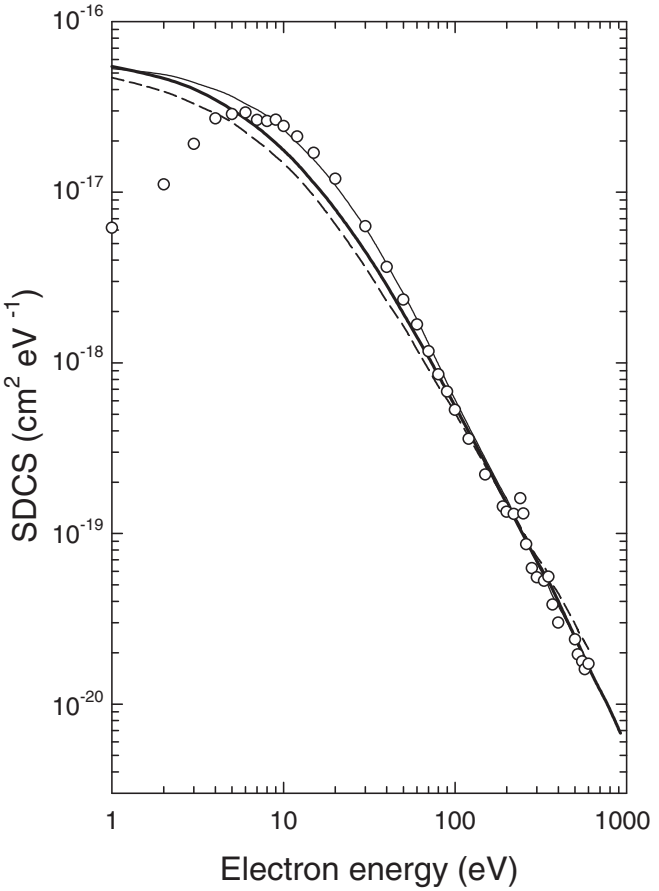

FIG. 7. Single-differential cross section for the electron emission from the uracil molecule following ionization by 1-MeV proton impact. Open circles, measured data [7]; dashed line, CDW-EIS [12]; thin solid line, CB1 [12]; thick solid line, present CTMC.

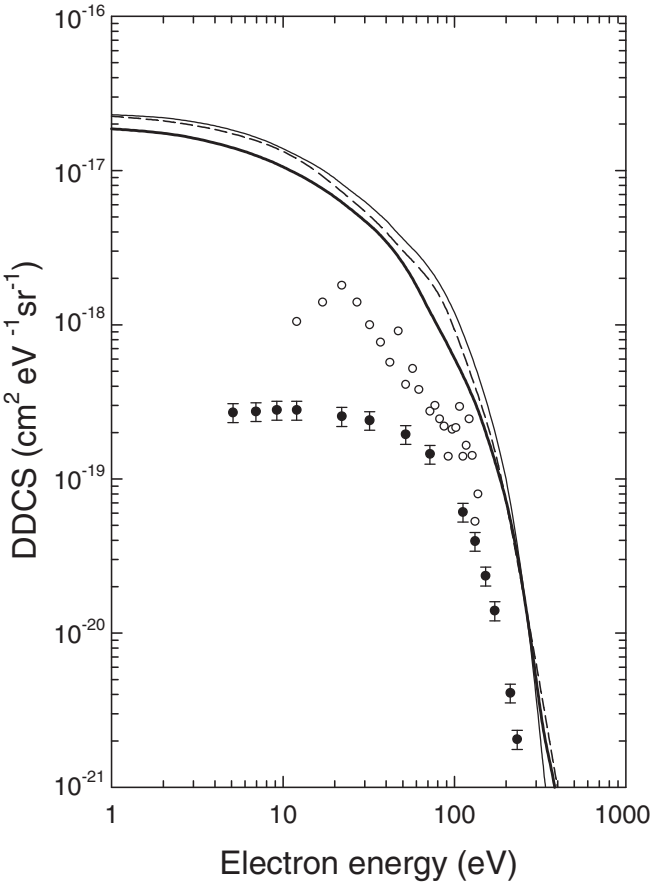

FIG. 8. Double-differential cross section for the electron emission from the uracil molecule following ionization by 100-keV proton impact. Closed circles with error bar, measured data [6]; dashed line, CDW-EIS [12]; thin solid line, CB1 [12]; open circles, CTMC results of Moretto-Capelle and Le Padellec [6]; thick solid line, present CTMC.

a function of the incident proton energy. Above 100 keV the theories behave similarly; they predict almost the same slope of the decrease of TCS with increasing energy. Our CTMC results are in good agreement with the experimental data of Itoh *et al.* [7]. Below 100 keV the theories strongly diverge with decreasing energy. Unfortunately, there exist no experimental data in this energy range except the value at 80 keV measured by Tabet *et al.* [3] which, however, seems to be too large regarding the tendency of the high-energy data. We note that the low-energy range is very interesting theoretically for the following reasons. With decreasing energy the applicability of the perturbation theories (CDW-EIS, CB1) becomes questionable. A better description is hoped from CTMC and CTMC-COB, as nonperturbative models. As far as CTMC-COB is concerned, it can be considered as a simplified CTMC method, and the validity of the approximations applied in the model is uncertain at low impact energies.

In the following we investigate the effect of the use of multicenter molecular potential. To analyze the effect, we repeated our DDCS calculations at 1 MeV using a simplified CTMC procedure in which the ionization cross section of the uracil is determined as a linear combination of the contributions of the constituent atoms of the molecule:

$$\frac{d^2\sigma}{d\epsilon\, \mathrm{d}\Omega} = \sum_{i=1}^{N_{\mathrm{MO}}} \sum_{k=1}^{N_i} \zeta_{ik} \frac{d^2\sigma_{ik}^{\mathrm{at}}}{d\epsilon\, \mathrm{d}\Omega}. \tag{20}$$

Here N_i is the number of atomic states contributing to the ith MO, $d^2\sigma_{ik}^{\mathrm{at}}/d\epsilon d\Omega$ is the DDCS for the electron emission from the kth atomic state in the ith MO, and ζ_{ik}'s are the electron population numbers at the atomic centers. We note that Galassi *et al.* [11] applied the same single-center (atomic) approximation in their quantum mechanical calculations.

Information about the effect of the multicenter molecular potential can be obtained by comparing DDCS based on the use of atomic potentials according to Eq. (20) with that based on the use of molecular potential. (In the following we refer to the two CTMC models as "atomic" and "molecular.") For a correct comparison, however, one has to take into account the large sensitivity of the cross section on the binding energies of the electrons in the MOs. This means that the atomic CTMC leads to comparable results with the molecular one only if the average value of the binding energies of the atomic states in a given MO is approximately equal to the binding energy of the

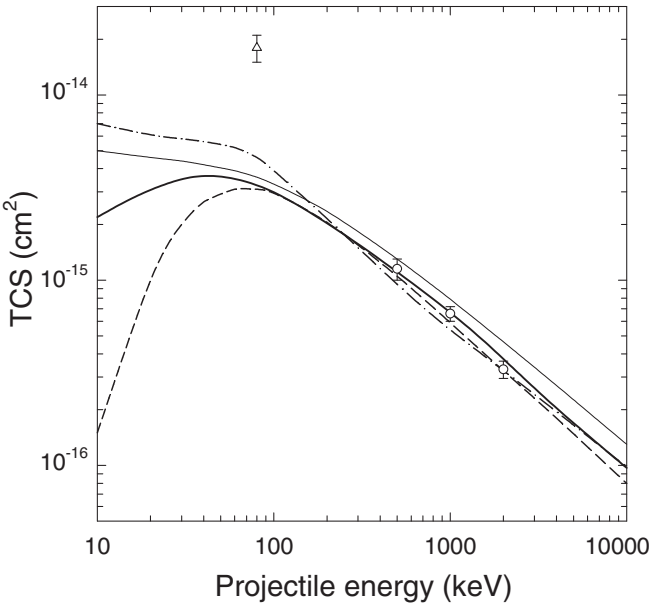

FIG. 9. Total cross section for the electron emission from the uracil molecule induced by protons as a function of the impact energy. (Experimental data) Open circles, Itoh *et al.* [7]; triangle, Tabet *et al.* [3]. (Theories) Dashed line, CDW-EIS [12]; thin solid line, CB1 [12]; dashed-dotted line, CTMC-COB [9]; thick solid line, present CTMC.

MO, i.e.,

$$E_i \approx \sum_{k=1}^{N_i} w_{ik}\, \varepsilon_{ik}. \tag{21}$$

Here ε_{ik}'s are the binding energies of the atomic states. As weighting factors we may use the normalized electron population numbers, $w_{ik} = \zeta_{ik} / \sum_{k=1}^{N_i} \zeta_{ik}$.

The condition Eq. (21), however, is not fulfilled in the case of *unperturbed* atomic states. In the molecule the states of an atom are strongly perturbed by the surrounding atoms leading to substantially reduced binding energies. We obtained approximate perturbed atomic binding energies by considering ε_{ik} in Eq. (21) as variables, and fitting the $\sum_{k=1}^{N_i} w_{ik}\, \varepsilon_{ik}$ values to E_i for the 21 valence shells of uracil. As MO binding energies and electron population numbers we used the data tabulated by Galassi *et al.* [11]. The best fit was achieved with the following perturbed binding energies (in eV): H($1s$), 13.84; C($2s$), 32.22; N($2s$), 34.12; O($2s$), 42.76; O($2p$), 10.03. For C($2p$) and N($2p$) a good fit was obtained by assuming two perturbed values: C($2p$), 8.00 and 16.26; N($2p$), 12.25 and 22.33.

We emphasize that the above procedure is very approximate; it ensures only the consistency of our analysis from energetical point of view.

For calculation of $d^2\sigma_{ik}^{\rm at}/d\epsilon {\rm d}\Omega$ in Eq. (20) we used our standard atomic CTMC code applying the Green-Sellin-Zachor screened potential [17]. The DDCS values obtained by the atomic and molecular CTMC model are compared in Fig. 10 at emission angles 15° and 165°. At 15° the two models resulted in almost the same DDCS values; the atomic model predicts slightly larger DDCS than the molecular model. At 165° the effect is large, the DDCS obtained by the atomic model is greatly reduced as compared to the molecular model, and differences up to a factor of 3 can be observed between the two approaches.

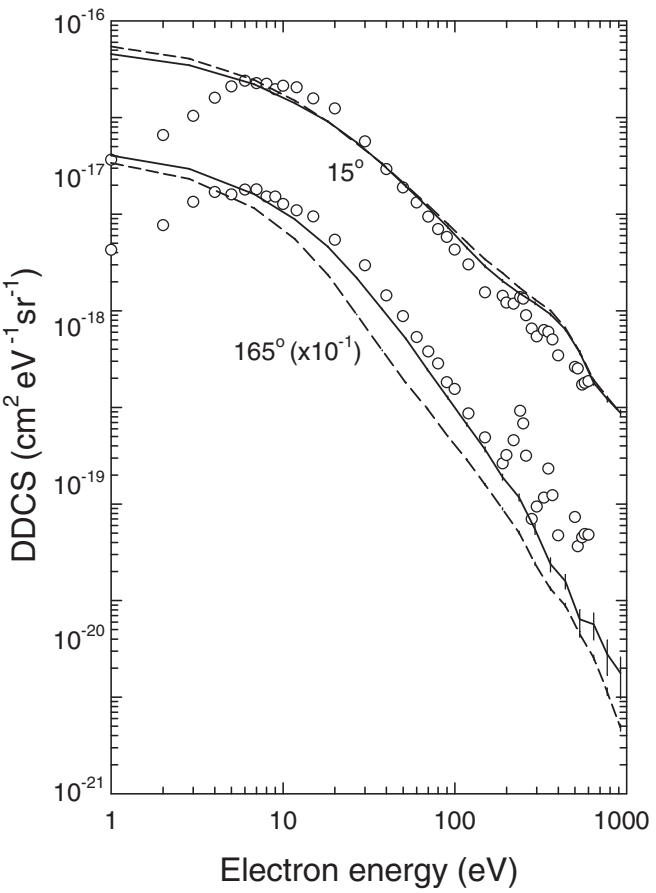

FIG. 10. DDCS for electron emission from the 1-MeV proton on uracil collisions. Solid lines, the present CTMC model; dashed lines, a simplified CTMC model based on the calculation of the individual contributions of the constituent atoms of the molecule according to Eq. (20). Experimental data, Itoh *et al.* [7].

A possible explanation for the enhancement of the backward electron emission in the case of the multicenter molecular potential is as follows. The backward emission can be viewed as a two-step process. In the first step the electron is ejected from the atom in the forward direction in the incoming phase of the collision. In the case of a free atom, in the second step the electron is scattered back by the target nucleus. In a molecule the probability of backscattering increases due to the more than one number of the scattering centers.

We note here an important consequence of the above finding. We may assume that the use of a multicenter molecular potential in the quantum mechanical calculations would lead also enhanced DDCS values at backward angles, i.e., it would shift up the CDW-EIS and CB1 curves seen in Fig. 5 for 120° and 165° emission angles. This means that the agreement between the experiment and theory would be improved for CDW-EIS; at the same time, it would be worsened for CB1. In other words, the good performance of CB1 in the description of the experimental data may be considered as accidental. This is

in accordance with the expectation, since CDW-EIS is a more justified ionization theory than CB1.

IV. CONCLUSIONS

We investigated the electron emission from the uracil molecule induced by fast proton impact using the CTMC method. We have shown that for 1-MeV impact energy CTMC provides integrated and differential cross section data that are comparable with those obtained by quantum mechanical calculations. Our CTMC results are in reasonable agreement with the experimental data. However, in spite of applying a multicenter molecular potential, CTMC could not resolve the large discrepancy found between the quantum mechanical models and the experiment for DDCS below 10 eV. In the same way, at 100-keV impact energy CTMC supports CDW-EIS and CB1, but it is in strong disagreement with the experiment and a previous CTMC model.

The comparison of the present CTMC results obtained for TCS with the predictions of other theories (CDW-EIS, CB1, CTMC-COB) shows a strong divergence of the models with decreasing impact energy. This calls the attention for the necessity of experiments at energies below 100 keV by which the performance of the theoretical models would be checked more efficiently than at higher impact energies.

Our simplified CTMC calculations made with atomic potentials showed the importance of using multicenter molecular potential in the description of the ionization process of the molecule, particularly regarding the electron emission at backward directions.

ACKNOWLEDGMENTS

This work was supported by the National Scientific Research Foundation (OTKA, Grant No. K109440) and the National Information Infrastructure Program (NIIF).

[1] B. Coupier *et al.*, Eur. Phys. J. D **20**, 459 (2002).
[2] J. de Vries, R. Hoekstra, R. Morgenstern, and T. Schlathölter, J. Phys. B **35**, 4373 (2002).
[3] J. Tabet, S. Eden, S. Feil, H. Abdoul-Carime, B. Farizon, M. Farizon, S. Ouaskit, and T. D. Märk, Phys. Rev. A **82**, 022703 (2010).
[4] A. N. Agnihotri, S. Kasthurirangan, S. Nandi, A. Kumar, M. E. Galassi, R. D. Rivarola, O. Fojon, C. Champion, J. Hanssen, H. Lekadir, P. F. Weck, and L. C. Tribedi, Phys. Rev. A **85**, 032711 (2012).
[5] A. N. Agnihotri *et al.*, J. Phys. B **46**, 185201 (2013).
[6] P. Moretto-Capelle and A. Le Padellec, Phys. Rev. A **74**, 062705 (2006).
[7] A. Itoh, Y. Iriki, M. Imai, C. Champion, and R. D. Rivarola, Phys. Rev. A **88**, 052711 (2013).
[8] M. C. Bacchus-Montabonel, M. Łabuda, Y. S. Tergiman, and J. E. Sienkiewicz, Phys. Rev. A **72**, 052706 (2005).
[9] H. Lekadir, I. Abbas, C. Champion, O. Fojón, R. D. Rivarola, and J. Hanssen, Phys. Rev. A **79**, 062710 (2009).
[10] I. Abbas, C. Champion, B. Zarour, B. Lasri, and J. Hanssen, Phys. Med. Biol. **53**, N41 (2008).
[11] M. E. Galassi, C. Champion, P. F. Weck, R. D. Rivarola, O. Fojón, and J. Hanssen, Phys. Med. Biol. **57**, 2081 (2012).
[12] C. Champion, M. E. Galassi, P. F. Weck, S. Incerti, R. D. Rivarola, O. Fojón, J. Hanssen, Y. Iriki, and A. Itoh, Nucl. Instrum. Methods B **314**, 66 (2013).
[13] Dž. Belkić, R. Gayet, J. Hanssen, and A. Salin, J. Phys. B **19**, 2945 (1986).
[14] D. S. F. Crothers and J. F. McCann, J. Phys. B **16**, 3229 (1983).
[15] R. Abrines and I. C. Percival, Proc. Phys. Soc. London **88**, 861 (1966).
[16] R. E. Olson and A. Salop, Phys. Rev. A **16**, 531 (1977).
[17] B. Sulik and K. Tőkési, Adv. Quantum Chem. **52**, 253 (2007).
[18] S. Kovács *et al.* (unpublished).
[19] C. Illescas, L. F. Errea, L. Méndez, B. Pons, I. Rabadán, and A. Riera, Phys. Rev. A **83**, 052704 (2011).
[20] A. E. S. Green, D. L. Sellin, and A. S. Zachor, Phys. Rev. **184**, 1 (1969).
[21] R. H. Garvey, C. H. Jackman, and A. E. S. Green, Phys. Rev. A **12**, 1144 (1975).
[22] C. O. Reinhold and C. A. Falcón, Phys. Rev. A **33**, 3859 (1986).
[23] T. van der Wijst, C. F. Guerra, M. Swart, F. M. Bickelhaupt, and B. Lippert, Chem. Eur. J. **15**, 209 (2009).
[24] L. Harsányi, A. Császár, and P. Császár, J. Mol. Struct., Theochem **137**, 207 (1986).